Eur. Phys. J. A (2017) **53**: 199
DOI 10.1140/epja/i2017-12394-2

THE EUROPEAN PHYSICAL JOURNAL A

Regular Article – Experimental Physics

Evaluation of cross sections for neutron interactions with ^{238}U in the energy region between 5 keV and 150 keV

I. Sirakov[1], R. Capote[2], O. Gritzay[3], H.I. Kim[4], S. Kopecky[5], B. Kos[6], C. Paradela[5], V.G. Pronyaev[7], P. Schillebeeckx[5,a], and A. Trkov[2]

[1] Institute for Nuclear Research and Nuclear Energy, BG-1784 Sofia, Bulgaria
[2] International Atomic Energy Agency, NAPC-Nuclear Data Section, A-1400 Vienna, Austria
[3] Institute for Nuclear Research, pr. Nauky, Kyiv, 03028, Ukraine
[4] Korea Atomic Energy Research Institute, Nuclear Data Center, Daejeon 34057, Republic of Korea
[5] European Commission, Joint Research Centre, B-2440 Geel, Belgium
[6] Jožef Stefan Institute, Jamova cesta 39, SI-1000 Ljubljana, Slovenia
[7] Atomsrandart, Rosatom State Corporation, Moscow, Russia

Received: 10 August 2017 / Revised: 12 September 2017
Published online: 18 October 2017

Communicated by R.K. Bhandari

Abstract. Cross sections for neutron interactions with ^{238}U in the energy region from 5 keV to 150 keV have been evaluated. Average total and capture cross sections have been derived from a least squares analysis using experimental data reported in the literature. The resulting cross sections have been parameterised in terms of average resonance parameters maintaining full consistency with results of optical model calculations by using a dispersive coupled channel optical model potential. The average compound partial cross sections have been expressed in terms of transmission coefficients by applying the Hauser-Feshbach statistical reaction theory including width-fluctuations. A generalized single-level representation compatible with the energy-dependent options of the ENDF-6 format has been applied using standard boundary conditions. The results have been transferred into a full ENDF-6 compatible data file.

1 Introduction

The status of evaluated data files for neutron interactions with ^{238}U in the resonance region is discussed in detail by Kopecky *et al.* [1]. Most of the evaluated data libraries refer for the unresolved resonance region (URR) to the work of Fröhner [2,3]. Fröhner's evaluation was obtained from an analysis of only energy dependent experimental cross section data without any adjustment to integral benchmark data. Nevertheless, in the energy region below 150 keV differences of more than 5% are observed [1] between the average capture cross sections in the main data libraries, *i.e.* ENDF/B-VII.1, JEFF-3.2 and JENDL-4, and the one recommended by Carlson *et al.* [4]. The latter was produced as part of the neutron standards project and results from a combined least squares analysis of experimental data available in the literature, including ratio measurements of different reactions. In addition, results of high resolution time-of-flight (TOF) total cross section measurements carried out by Harvey *et al.* [5] have not been included in previous evaluations for the URR, *e.g.* in the evaluation performed by Fröhner [2,3], Maslov *et al.* [6] and Courcelle *et al.* [7]. The data of Harvey *et al.* [5] were analysed by Derrien *et al.* [8] to derive average total cross sections between 10 keV and 100 keV. This shows the need of a new evaluation based on well documented experimental data. The present evaluation includes the results of Derrien *et al.* [8], as well as the capture data obtained from TOF experiments at the LANSCE [9], GELINA [10] and n_TOF [11,12] facilities, which were not available for previous evaluation projects.

The results of the present work have been included in the evaluated data file for neutron induced reactions on ^{238}U reported by Capote *et al.* [13]. The file was developed at the IAEA as part of the CIELO (Collaborative International Evaluated Library Organization) project [14,15]. The objective of CIELO is to produce general purpose nuclear data files that are world-wide recognised with a focus on six high-priority nuclides, *i.e.* ^{1}H, ^{16}O, ^{56}Fe, ^{235}U, ^{238}U and ^{239}Pu. The evaluation procedures for CIELO should as much as possible be based on an analysis of

[a] e-mail: peter.schillebeeckx@ec.europa.eu (corresponding author)

Table 1. Experimental total cross section data used to derive an average total cross section $\overline{\sigma}_{tot}$ for neutron induced reactions on ^{238}U in the energy region between 5 keV and 150 keV. The fully correlated uncertainty u_c utilised in the analysis is given together with the energy region of the data employed in the analysis.

	Ref.	u_c	Method	Energy region	EXFOR entry
Whalen *et al.* (1971)	[18]	$u_c = 0.1b$	TOF	100 keV–150 keV	10009
Konovov *et al.* (1973)	[19]	$0.1b \leq u_c \leq 0.6b$	TOF	5 keV–82 keV	40328
Poenitz *et al.* (1981, 1983)	[20,21]	$0.08b \leq u_c \leq 0.18b$	TOF	48 keV–140 keV	10935
Tsubone *et al.* (1984)	[22]	$u_c = 0.05b$	Fe-filtered beam + TOF	25 keV–140 keV	21813
Bokhovko *et al.* (1990)	[23]	$u_c = 0.1b$	TOF	10 keV–110 keV	41016
Derrien *et al.* (2004)	[8]	$u_c = 0.03b$	TOF	10 keV–90 keV	

experimental microscopic cross section data such that the recommended cross sections are not biased by results of integral benchmark experiments.

2 Least squares analysis of average total and capture cross section data

Average total $\overline{\sigma}_{tot}$ and capture $\overline{\sigma}_{\gamma}$ cross sections between 5 keV and 150 keV were derived from a least squares adjustment to experimental data reported in the literature. The generalised least squares code GMA developed by Poenitz [16] was used. This code, which is named after Gauss, Markov and Aitken, is available at the IAEA [17].

2.1 Average total cross section

The average total cross section $\overline{\sigma}_{tot}$ obtained in this work is based on an analysis of the data in table 1. All these data were obtained from TOF experiments [8,18–23]. Tsubone *et al.* [22] reduced the background by performing TOF experiments using a Fe-filtered neutron beam. For all these data sets a correction for self-shielding is specified in the papers or reports that describe the experiments and analysis procedures. Only data sets for which at least the total uncertainties are given were included in the analysis. An ideal GMA analysis relies on data for which the individual uncertainty components, in particular correlated and uncorrelated components, are given. When this information could not be retrieved from the papers or the EXFOR data library [24], the covariance matrix was constructed based on one correlated component, due to a normalisation uncertainty, combined with an uncorrelated uncertainty maintaining as much as possible the reported total uncertainty. If only the uncorrelated component is reported then a normalisation uncertainty was added. No correlation between results of different experiments was assumed.

The resulting average total cross section $\overline{\sigma}_{tot}$ is listed in table 2. This $\overline{\sigma}_{tot}$ is compared in fig. 1 with the experimental data that were used in the analysis and the cross section derived from the JEF-2.2 library. The latter is based on the analysis of Moxon *et al.* [25] in the resolved resonance region (RRR) and the work of Fröhner [2,3] in the URR. There is a very good agreement between the results of the GMA analysis and the total cross section recommended in JEF-2.2.

2.2 Average capture cross section

The average capture cross section $\overline{\sigma}_{\gamma}$ was derived by combining the capture data used by Carlson *et al.* [4] with those of Ullmann *et al.* [9], Kim *et al.* [10], Mingrone *et al.* [11] and Wright *et al.* [12].

The data used by Carlson *et al.* [4], which are also listed in ref. [26], include: 11 absolute $^{238}\mathrm{U}(\mathrm{n},\gamma)$, 2 shape $^{238}\mathrm{U}(\mathrm{n},\gamma)$, 2 absolute $^{238}\mathrm{U}(\mathrm{n},\gamma)/^{6}\mathrm{Li}(\mathrm{n},\alpha)$ ratio, 5 absolute $^{238}\mathrm{U}(\mathrm{n},\gamma)/^{10}\mathrm{B}(\mathrm{n},\alpha_1)$ ratio, 4 shape $^{238}\mathrm{U}(\mathrm{n},\gamma)/^{10}\mathrm{B}(\mathrm{n},\alpha_1)$ ratio, 4 absolute $^{238}\mathrm{U}(\mathrm{n},\gamma)/^{10}\mathrm{B}(\mathrm{n},\alpha)$ ratio, 9 absolute $^{238}\mathrm{U}(\mathrm{n},\gamma)/^{197}\mathrm{Au}(\mathrm{n},\gamma)$ ratio, 1 shape $^{238}\mathrm{U}(\mathrm{n},\gamma)/^{197}\mathrm{Au}(\mathrm{n},\gamma)$ ratio, 5 absolute $^{238}\mathrm{U}(\mathrm{n},\gamma)/^{235}\mathrm{U}(\mathrm{n},\mathrm{f})$ ratio, 6 shape $^{238}\mathrm{U}(\mathrm{n},\gamma)/^{235}\mathrm{U}(\mathrm{n},\mathrm{f})$ ratio and 1 shape $^{238}\mathrm{U}(\mathrm{n},\gamma)/^{239}\mathrm{Pu}(\mathrm{n},\mathrm{f})$ ratio measurements. The $^{238}\mathrm{U}(\mathrm{n},\gamma)$ cross section data of Ullmann *et al.* [9] and Wright *et al.* [12] result from measurements with a total absorption detector. Kim *et al.* [10] and Mingrone *et al.* [11] applied the total energy detection principle using a set of C_6D_6 liquid scintillators in combination with the pulse height weighting technique.

The resulting average capture cross section $\overline{\sigma}_{\gamma}$ is reported in table 3. Figure 2 compares this cross section with the one of Carlson *et al.* [4], the data of refs. [9–12] and the cross section derived from the JEF-2.2 library. The present results are very close to the cross section derived from the JEF-2.2 library. Below 10 keV the cross section obtained in this work shows a similar structure as the experimental data of refs. [9–12] and the cross section in JEF-2.2. The absence of such a structure in the cross section recommended by Carlson *et al.* [4] is due to the limited number of high-energy resolution data combined with a sparse energy grid involved in the work of Carlson *et al.* [4]. Above 10 keV the main difference with the cross section of Carlson *et al.* [4] is a reduction in the uncertainty by about 40%. Similar conclusions were already drawn by Kim *et al.* [10] from a GMA analysis combining the data used by Carlson *et al.* [4] with only their data. In fact the results obtained by Kim *et al.* [10] are very close to those obtained in this work. Differences with the previous evaluation of Carlson *et al.* [4] are predominantly due

Table 2. Average total cross section $\overline{\sigma}_{tot}$, its uncertainty, and correlation coefficient $\rho(\overline{\sigma}_{tot,i}, \overline{\sigma}_{tot,j})$ derived from a least squares analysis using the data of refs. [8,18–23].

E/keV	$\overline{\sigma}_{tot}$/b	$\rho(\overline{\sigma}_{tot,i}, \overline{\sigma}_{tot,j}) \times 100$																	
5.5	19.43 ± 2.25	100	43	9	6	1	1	1	1	1	1	1	1	1	1	0	0	0	0
6.5	18.72 ± 2.11		100	50	11	1	1	1	1	1	1	1	1	1	1	0	0	0	0
7.5	16.49 ± 2.19			100	54	1	1	0	0	0	1	0	0	0	1	0	0	0	0
8.5	16.06 ± 1.79				100	3	0	0	0	1	1	0	1	1	1	0	0	0	0
9.5	14.646 ± 0.078					100	7	7	6	9	12	8	10	11	11	9	7	2	1
15	15.129 ± 0.053						100	10	9	13	18	13	16	16	17	13	10	2	2
20	14.674 ± 0.051							100	12	13	17	13	16	16	17	13	10	3	2
24	13.943 ± 0.030								100	15	16	11	18	16	16	12	9	10	10
30	13.780 ± 0.034									100	22	16	21	21	21	17	13	3	3
45	13.062 ± 0.025										100	31	27	27	29	22	17	4	4
55	12.994 ± 0.034											100	31	18	21	16	12	3	3
65	12.480 ± 0.019												100	43	28	20	15	5	4
75	12.249 ± 0.023													100	51	26	16	6	6
85	12.178 ± 0.024														100	42	27	7	7
95	12.026 ± 0.032															100	29	5	4
100	11.785 ± 0.039																100	8	6
120	11.611 ± 0.047																	100	32
150	11.310 ± 0.048																		100

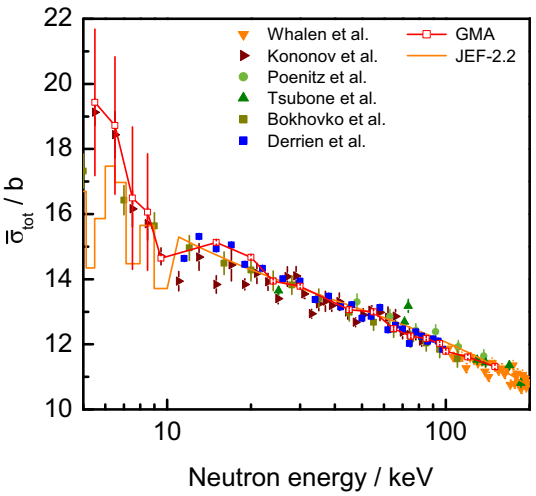

Fig. 1. Average total cross section $\overline{\sigma}_{tot}$ for neutron interactions with ^{238}U as a function of neutron energy. The experimental data of Whalen *et al.* [18], Kononov *et al.* [19], Poenitz *et al.* [20,21], Tsubone *et al.* [22], Bokhovko *et al.* [23] and Derrien *et al.* [8] are compared with the results of a GMA analysis of these data and the one of JEF-2.2. The latter is based on the evaluation of Moxon [25] in the RRR and the evaluation performed by Fröhner [2,3] in the URR.

to the GELINA data of Kim *et al.* [10], which have a substantial lower uncertainty compared to those of Ullman *et al.* [9], Mingrone *et al.* [11] and Wright *et al.* [12].

Above 100 keV the data of Ullman *et al.* [9] and Mingrone *et al.* [11] deviate from both the results of Carlson *et al.* [4] and the present GMA analysis that includes these data. Ullman *et al.* [9] remark that their data suffer from bias effects in the region of the strong Al resonances at 36 keV, 88 keV and 104 keV. The differences with the results of Carlson *et al.* [4] around 100 keV are not discussed by Mingrone *et al.* [11]. It should be noticed, however, that similar deviations can be observed (see ref. [27]) between the ^{197}Au(n, γ) cross section data obtained from measurements at the n_TOF facility in ref. [28] and the ^{197}Au(n, γ) cross section recommended by Carlson *et al.* [4], which was confirmed by the GELINA data of Massimi *et al.* [27].

3 Parameterisation of the cross sections in the URR by average resonance parameters

In the URR average compound cross sections can be parameterised in terms of transmission coefficients by means of the Hauser-Feshbach statistical reaction theory with width fluctuations, following various schemes for the fluctuation correction factor [29–32]. The width fluctuation correction factor approach used in this work has been the ENDF statistical integration with a Gauss quadrature scheme [33], which is both equivalent to an accurately calculated Dresner integral and compatible with the ENDF-6 format/model. More details can be found in refs. [34,27].

The average total and capture cross sections are expressed as a function of the scattering radius $R'(E)$, neutron strength functions $S_\ell(E)$ and capture transmission coefficients $T_\gamma^{J^\pi}(E)$, with ℓ the angular momentum and J^π the spin and parity of the compound nucleus. In most cases the scattering radius and neutron strength functions depend only weakly on the energy of the incoming neutron.

Table 3. Average capture cross section $\overline{\sigma}_\gamma$, its uncertainty, and correlation coefficient $\rho(\overline{\sigma}_{\gamma,i}, \overline{\sigma}_{\gamma,j})$ derived from a least squares analysis using the capture data recommended by Carlson *et al.* [4] and the data of refs. [9–12].

E/keV	$\overline{\sigma}_\gamma$/b	$\rho(\overline{\sigma}_{\gamma,i}, \overline{\sigma}_{\gamma,j}) \times 100$																	
5.5	0.8904 ± 0.0085	100	33	23	28	30	34	30	34	32	37	30	31	29	25	18	15	16	16
6.5	0.8427 ± 0.0090		100	41	31	30	33	29	33	32	36	30	31	29	24	18	15	16	15
7.5	0.7474 ± 0.0073			100	46	30	33	27	32	30	34	28	29	27	23	17	14	15	14
8.5	0.6442 ± 0.0055				100	34	36	27	34	32	35	28	29	28	24	17	15	15	15
9.5	0.6844 ± 0.0066					100	38	33	38	36	41	34	35	33	28	21	17	18	17
15	0.5910 ± 0.0044						100	38	46	44	49	40	41	39	33	24	21	22	21
20	0.5299 ± 0.0051							100	43	38	44	36	37	36	30	23	19	21	21
24	0.4718 ± 0.0035								100	51	52	43	44	41	36	29	25	26	27
30	0.4345 ± 0.0034									100	52	43	44	42	37	31	26	28	28
45	0.3574 ± 0.0028										100	51	48	46	40	31	27	28	27
55	0.2895 ± 0.0026											100	50	37	35	27	23	25	25
65	0.2449 ± 0.0022												100	52	33	28	24	26	24
75	0.2114 ± 0.0020													100	49	27	21	25	23
85	0.1879 ± 0.0020														100	49	36	23	23
95	0.1815 ± 0.0023															100	67	29	24
100	0.1788 ± 0.0025																100	39	25
120	0.1637 ± 0.0021																	100	35
150	0.1411 ± 0.0016																		100

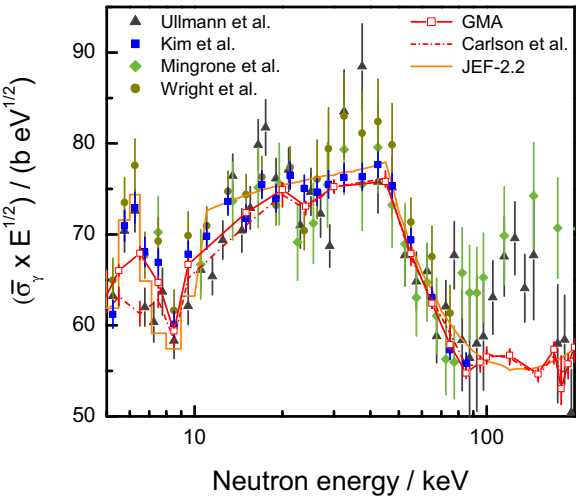

Fig. 2. Average capture cross section $\overline{\sigma}_\gamma$ for ^{238}U(n, γ) as a function of neutron energy. The experimental data of Ullmann *et al.* [9], Kim *et al.* [10], Mingrone *et al.* [11] and Wright *et al.* [12] are compared with the results of a GMA analysis of these data combined with the data used by Carlson *et al.* [4]. The result of the GMA analysis is compared with the one of Carlson *et al.* [4] and JEF-2.2. The latter is based on the evaluation of Moxon [25] in the RRR and the evaluation performed by Fröhner [2,3] in the URR.

This dependence can be derived from results of optical model calculations [34,35]. The energy dependence of the transmission coefficient for the capture channel $T_\gamma^{J^\pi}(E)$ can be parameterised by [34]

$$T_\gamma^{J^\pi}(E) = T_{\gamma,0}^{J^\pi} W_{T_\gamma}^{J^\pi}(E), \quad (1)$$

where $T_{\gamma,0}^{J^\pi} = T_\gamma^{J^\pi}(E = 0)$ is the capture transmission coefficient at zero neutron energy. The energy dependent term $W_{T_\gamma}^{J^\pi}(E)$ is determined from the definition of $T_\gamma^{J^\pi}(E)$ as a sum of single-channel photon transmission coefficients $T_{XL}(\epsilon_\gamma)$. The summation (integration) is over the transition types X, multipolarities L and photon energies ϵ_γ of the primary γ-rays that deexcite the compound nucleus to lower-lying states.

Two models have been tried in the analysis. The first one assumed that the transmission coefficient $T_{E1}(\epsilon_\gamma)$ of the predominating electric dipole transition is represented in a Lorentzian approximation of the photo-absorption cross section by a Giant Dipole Resonance (GDR) as proceeded in refs. [34,27]. The alternative model tried (employed for instance in the JENDL-4.0 evaluation) was the energy independent option for the average radiation width $\overline{\Gamma}_\gamma^\pi$ rather than its energy dependence by the GDR model. The constant radiation width has performed significantly better with the Gilbert-Cameron level density in optimising capture transmission coefficients on the capture data up to 150 keV and has ultimately been chosen in the analysis. The J-dependence of $T_\gamma^{J^\pi}$ can be determined from the known J-dependence of the level density with the common assumption that the effective radiation widths only depend on the parity [34]. Thus, independent parameters for the capture channel might be any two $T_{\gamma,0}^{J^\pi}$-values that belong to different parities (even and odd ℓ), *e.g.* $T_{\gamma,0}^{(I+1/2)^+}$ and $T_{\gamma,0}^{(I+1/2)^-}$, where I is the spin of the target nucleus.

Hence, independent parameters to determine the average total and capture cross section in the URR are the scattering radius, neutron strength functions and the

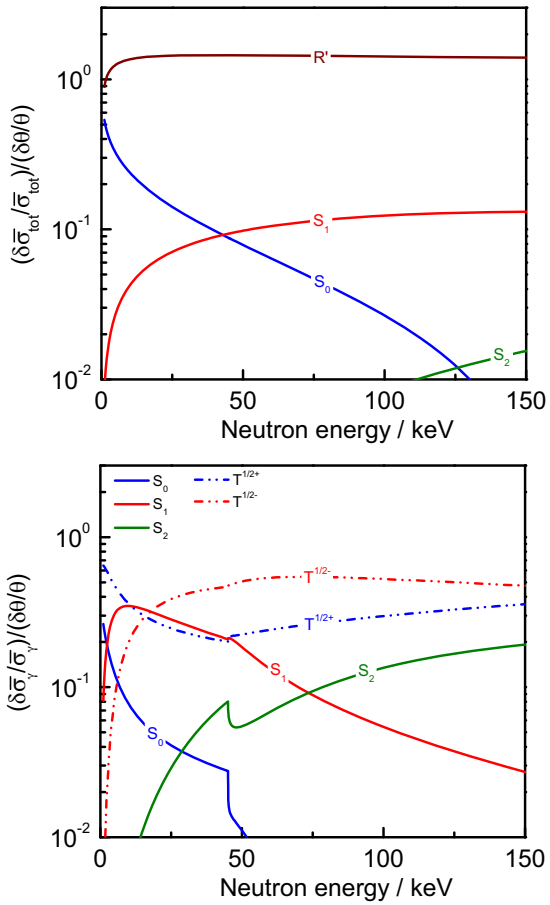

Fig. 3. Sensitivity of the average total $(\delta\overline{\sigma}_{tot}/\overline{\sigma}_{tot})/(\delta\theta/\theta)$ and the average capture cross section $(\delta\overline{\sigma}_{\gamma}/\overline{\sigma}_{\gamma})/(\delta\theta/\theta)$ to the parameter θ as a function of neutron energy. The parameter θ represents the scattering radius, the neutron strength functions $S_{\ell=0,1,2}$ and γ-ray transmission coefficients $T_{\gamma,0}^{1/2^+}$ and $T_{\gamma,0}^{1/2^-}$.

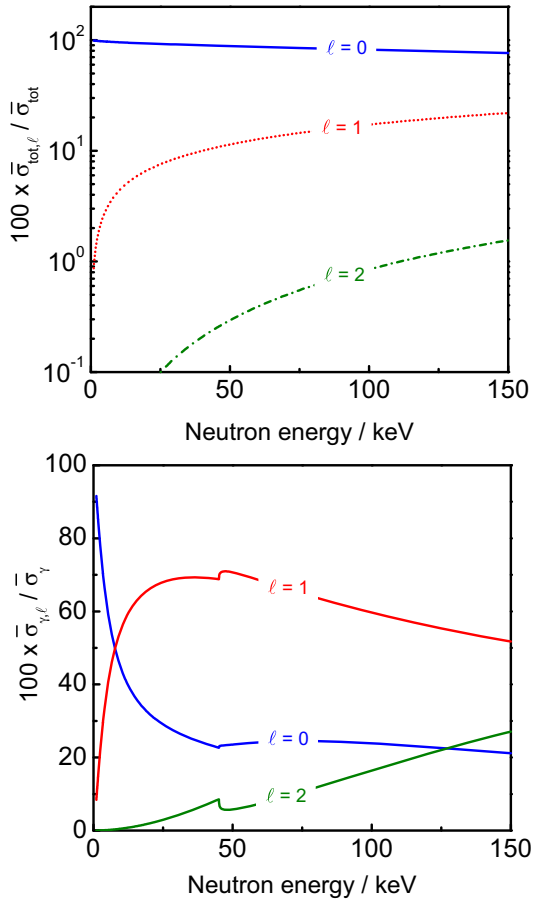

Fig. 4. Relative contribution of s-, p- and d-wave neutrons ($\ell = 0$, 1 and 2) to the average total $\overline{\sigma}_{tot}$ and capture $\overline{\sigma}_{\gamma}$ cross section for ^{238}U as a function of neutron energy.

capture transmission coefficients. These quantities at zero energy are denoted as constants by R', $S_{\ell=0,1,2}$, $T_{\gamma,0}^{1/2^+}$ and $T_{\gamma,0}^{1/2^-}$. The sensitivities of the average total and capture cross section to the scattering radius R', strength functions $S_{\ell=0,1,2}$ and to the capture transmission coefficients $T_{\gamma,0}^{1/2^+}$ and $T_{\gamma,0}^{1/2^-}$ are shown in fig. 3 as a function of neutron energy. The dependences in fig. 3 reveal that the total cross section is mainly sensitive to the scattering radius R' and the s-wave neutron strength function S_0. The capture cross section is mainly sensitive to the capture transmission coefficients $T_{\gamma,0}^{1/2^+}$ and $T_{\gamma,0}^{1/2^-}$ and to the p-wave neutron strength function S_1. The decreasing sensitivity to the s-wave strength function and increasing sensitivity to the p-wave parameters with increasing energy follow from the relative contribution of the partial waves to the average total and capture cross sections, shown in fig. 4.

It is known that through the W-factor in eq. (1) the capture transmission coefficients and the capture cross section additionally depend on the s-wave level spacing at zero neutron energy, denoted by D_0. The latter is usually used to determine the level density parameter and, consequently, the energy dependence in the level density formula. In the URR, however, the capture cross section sensitivity to D_0 (keeping $T_{\gamma,0}^{1/2^+}$ and $T_{\gamma,0}^{1/2^-}$ intact) ranges from -0.04% at 5 keV to -1.6% at 150 keV, and therefore is practically negligible. Hence, the average level spacing D_0 can not reliably be determined from its optimisation to average capture cross section data in the URR and has to be adopted or deduced in another way, as discussed in sect. 4.

The transmission coefficient for an inelastic scattering channel $T_{c'}$ is approximated by the transmission coefficient for an elastic neutron channel T_c, provided that c has the same orbital momentum and the same kinetic channel energy as c'. Since only the first inelastic level is considered in the URR, one has

$$T_{c'(\ell')}(E) = T_{c(\ell=\ell')}(E - E_t), \tag{2}$$

with E_t being the inelastic threshold energy, and ℓ and ℓ' the orbital momentum of c and c', respectively.

The average total and capture cross sections resulting from the GMA analysis were parameterised in terms of average resonance parameters maintaining consistency with the results of optical model (OM) calculations re-

Table 4. The scattering radius, neutron strength functions $S_{\ell=0,1}$ and capture transmission coefficients, $T_{\gamma,0}^{1/2^-}$ and $T_{\gamma,0}^{1/2^+}$, at zero energy derived from the average cross section data in table 2 and table 3. The uncertainties and correlation matrix are also given. The neutron strength function $S_2 = 1.376 \times 10^{-4}$ was adopted from the DCCOM.

	θ	$\rho(\theta,\theta') \times 100$				
R'/fm	9.483 ± 0.020	100	−70	−86	75	−37
$S_0/10^{-4}$	1.064 ± 0.015		100	46	−49	30
$S_1/10^{-4}$	1.641 ± 0.033			100	−82	37
$T_{\gamma,0}^{1/2^+}/10^{-3}$	6.60 ± 0.14				100	−31
$T_{\gamma,0}^{1/2^-}/10^{-3}$	6.37 ± 0.07					100

ported by Capote *et al.* [36]. The procedure that was applied to evaluate the cross section data in the URR for ^{232}Th [34] and ^{197}Au [27,35] has been followed. The DCCOM potential of refs. [37,38] was used for the optical model calculations with the coupled-channel OPTMAN code [39,40] incorporated into the EMPIRE system [41]. Neutron strength functions $S_0(E)$, $S_1(E)$, and $S_2(E)$ that correspond to the OM data have been obtained so as to reproduce the compound formation cross sections of the DCCOM with the optical model parameters from RIPL 2412 [42]. The energy dependence of the direct inelastic scattering cross section was adopted from the same DCCOM calculations [36], while the energy dependence of the hard-sphere potential scattering radius $R'(E)$, which corresponds to the OM calculations, was derived from the shape elastic cross section of the DCCOM. More details about an ENDF URR model, which is equivalent to the OM with respect to the non-fluctuating cross sections (*i.e.*, the total, shape elastic and compound formation one), can be found in refs. [34,35].

The smooth and weak energy dependences obtained from the DCCOM for the scattering radius $R'(E)$ and neutron strength functions $S_\ell(E)$ were parameterized by second order polynomials. The resulting scattering radius R' and neutron strength functions $S_{\ell=0,1,2}$ at zero energy were used as initial fit parameters. The data sensitivity to S_2 was not sufficient for a reliable optimisation. Therefore, the strength function for d-wave neutrons was fixed to $S_2 = 1.376 \times 10^{-4}$ as derived from the DCCOM.

The final parameters together with their uncertainty and correlation matrix are listed in table 4. The covariance matrix was obtained by conventional uncertainty propagation of the covariance data in table 2 and table 3. The scattering radius at zero energy derived from the DCCOM ($R' = 9.6028$ fm) required a small adjustment. The adjusted radius $R' = (9.483 \pm 0.020)$ fm is fully consistent with the scattering radius $R' = 9.48$ fm that was used for a resonance shape analysis in the RRR by Kim *et al.* [10]. The initial strength functions S_0 and S_1 at zero energy derived from the DCCOM were practically not changed. The final values $S_0 = (1.064 \pm 0.015) \times 10^{-4}$ and $S_1 = (1.641 \pm 0.033) \times 10^{-4}$ are within the uncertainties in very good agreement with the strengths functions derived from a statistical analysis of resolved resonance parameters: $S_0 = (1.025 \pm 0.047) \times 10^{-4}$ and $S_1 = (1.652 \pm 0.046) \times 10^{-4}$ reported by Derrien *et al.* [43] and $S_0 = (1.03 \pm 0.05) \times 10^{-4}$ and $S_1 = (1.70 \pm 0.20) \times 10^{-4}$ by Courcelle *et al.* [7]. Derrien *et al.* [43] and Courcelle *et al.* [7] used the same resonance parameter file for their analysis. They are also consistent with the strength functions recommended in the RIPL library [42], *i.e.* $S_0 = (1.03 \pm 0.08) \times 10^{-4}$ and $S_1 = (1.6 \pm 0.2) \times 10^{-4}$. The total and capture cross sections calculated with the parameters in table 4 are shown in fig. 5 and fig. 6, respectively.

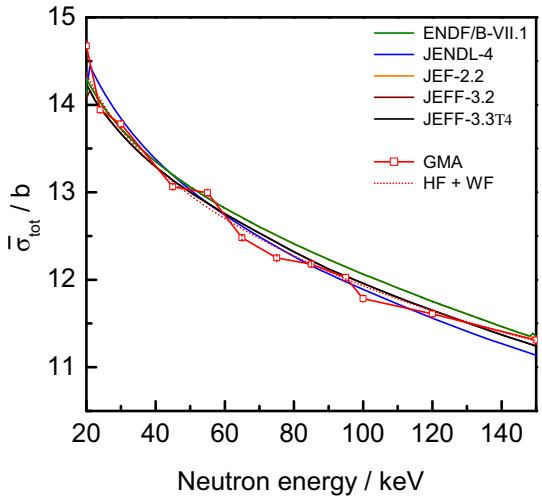

Fig. 5. Average total cross section $\overline{\sigma}_{tot}$ for neutron interactions with ^{238}U as a function of neutron energy. The result of a GMA analysis and the cross section derived from the average parameters in table 4 are compared with the total cross sections recommended in other data libraries, *i.e.* ENDF/B-VII.1, JENDL-4.0, JEF-2.2, JEFF-3.2 and JEFF-3.3T4.

4 An ENDF-6 compatible data file for energies between 20 keV and 150 keV

The results obtained in this work were used to produce an evaluated data file for neutron interactions with ^{238}U in the URR, from 20 keV to 149 keV. The boundary between the RRR and URR was kept at 20 keV, as in the file produced by Derrien *et al.* [43]. It should be noted that no substantial difference was found in the interpretation of integral benchmark experiments by reducing the upper

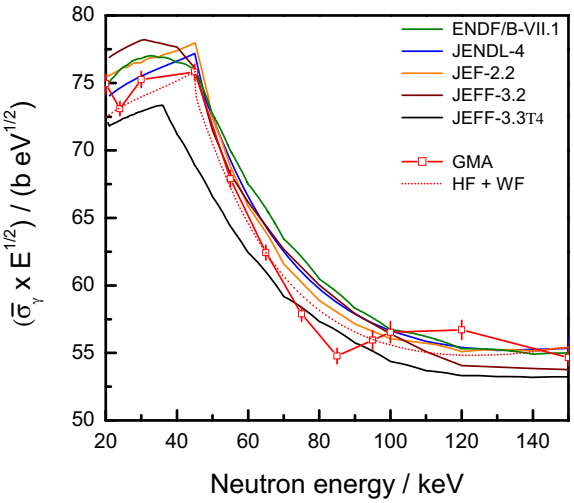

Fig. 6. Average capture cross section $\overline{\sigma}_\gamma$ for ^{238}U(n, γ) as a function of neutron energy. The result of a GMA analysis and the cross section derived from the average parameters in table 4 are compared with the capture cross sections recommended in other data libraries, *i.e.* ENDF/B-VII.1, JENDL-4.0, JEF-2.2, JEFF-3.2 and JEFF-3.3T4.

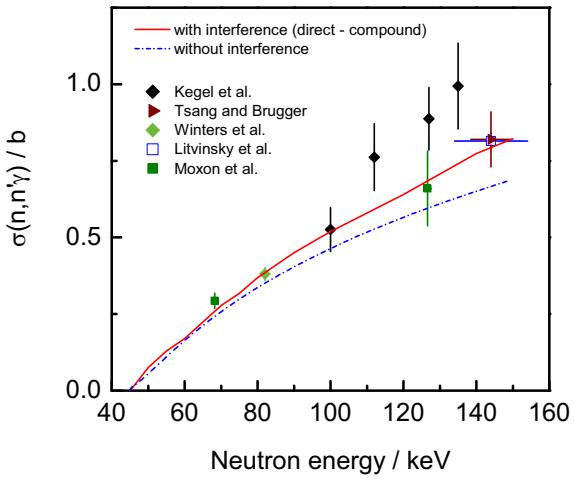

Fig. 7. Inelastic scattering cross section of ^{238}U as a function of neutron energy. The experimental data of Kegel *et al.* [45], Tsang and Brugger [46], Winters *et al.* [47], Litvinsky *et al.* [48] and Moxon *et al.* [49] are compared with the cross section calculated with and without accounting for the interference between the contributions of the direct- and of the compound reaction model. More information on the interference effect can be found in ref. [44].

limit of the RRR to 10 keV. More details on the effect of the upper boundary for the RRR can be found in ref. [1].

The average total and capture cross section resulting from the GMA analysis were adopted in file 3 with the LSSF=1 option as infinitely dilute total and capture cross sections, respectively. The inelastic neutron scattering cross section data of Capote *et al.* [36], which include compound-direct interference effects as discussed by Kawano *et al.* [44], were also adopted in file 3 by modifying the calculated infinitely dilute inelastic cross section based on both resonance parameters (ENDF-6 single orbital representation of the inelastic neutron widths) and the direct inelastic cross section from the DCCOM. The approximated impact of the compound-direct interference effect is illustrated in fig. 7. In this figure the experimental data of refs. [45–49] are compared with two calculated cross sections. For both calculations the inelastic scattering contributions determined by the direct as well as by the compound reaction model are considered. However, only for the cross section represented with the full line the interference between the two contributions is taken into account. This interference is at the expense of the remaining compound partial cross sections, predominantly the compound elastic one, so that the compound nucleus formation cross section is conserved. An overview on parameterising the collision matrix and processing compound interactions in the presence of direct reactions in the URR is in preparation [50]. The small average unresolved fission cross section of the order of 0.1 mb was adopted from an estimation by Trkov [51]. This estimation, which results in a more reasonable trend at the URR boundaries [13], was based on available low-resolution sub-threshold fission cross section data, particularly those of Slovacek *et al.* [52].

The average parameters listed in table 4 were used to produce an ENDF-6 compatible file 2, which is required for accurate self-shielding calculations. Conversion into the ENDF-6 format requires that the transmission coefficients $T_c^{J^\pi}$ are translated into effective partial widths $\overline{\Gamma}_c^{J^\pi}$ by means of the following relation:

$$T_c^{J^\pi} = 2\pi \frac{\overline{\Gamma}_c^{J^\pi}}{D^J}\,, \tag{3}$$

where c may be any entrance or exit, single or lumped, channel and D^J is the level spacing. The level spacing is related to the level density ρ^J by $D^J = 1/\rho^J$. For the capture channels eq. (3) becomes

$$T_\gamma^{J^\pi} = 2\pi \frac{\overline{\Gamma}_\gamma^{\pi}}{D^J}\,. \tag{4}$$

Two file versions have been tested in order to assign low-energy values for the s-wave level spacing, $D_0 = D^{1/2}(E = 0)$, and the s-wave radiation width, $\overline{\Gamma}^+_{\gamma,0} = \overline{\Gamma}^+_\gamma(E = 0)$, taking into account their relation with the optimised parameter

$$T_{\gamma,0}^{1/2^+} = 2\pi \frac{\overline{\Gamma}^+_{\gamma,0}}{D_0}\,. \tag{5}$$

In addition, as mentioned in sect. 3, energy independent radiation widths $\overline{\Gamma}^+_\gamma = \overline{\Gamma}_\gamma(\ell = 0, 2)$ and $\overline{\Gamma}^-_\gamma = \overline{\Gamma}_\gamma(\ell = 1)$ were chosen rather than their GDR energy dependence for the better χ^2-optimization.

In a first version the value of $\overline{\Gamma}_\gamma(\ell = 0) = 22.5$ meV resulting from a resonance shape analysis of transmission and capture data below 1.2 keV by Kim *et al.* [10] was

Table 5. Spectrum averaged total cross section based on the data reported in this work compared with experimental results reported by Livinsky *et al.* [48] and Pham *et al.* [58].

	Ref.	Most probable energy	Spectrum averaged cross section	
			Exp. data	This work
Litvinsky *et al.*	[48]	54 keV	(13.343 ± 0.051) b	(13.27 ± 0.05) b
(EXFOR Entry = 40924)		144 keV	(11.551 ± 0.022) b	(11.70 ± 0.05) b
Pham *et al.*	[58]	54 keV	(13.31 ± 0.11) b	(13.10 ± 0.05) b
(EXFOR Entry = 31457)		144 keV	(11.52 ± 0.11) b	(11.43 ± 0.05) b

adopted. Using the parameters of table 4 together with eq. (5) this corresponds to $D_0 = 21.4$ eV and $\overline{\Gamma}_\gamma(\ell = 1) = 21.7$ meV. In a second version an effective energy independent radiation width $\overline{\Gamma}_\gamma(\ell = 0)$ for the energy region between 20 keV and 150 keV was obtained after projecting the value of 22.5 meV from zero energy to a mid-energy point of 75 keV assuming a GDR energy dependence and obtaining $\overline{\Gamma}_\gamma(\ell = 0) = 23.32$ meV. This value is in agreement with the one recommended in RIPL 2412 [42], *i.e.* $\overline{\Gamma}_\gamma(\ell = 0) = (23.6 \pm 0.8)$ meV. The GDR parameters for the compound nucleus of ^{238}U + n was adopted from Holmes *et al.* [53]. A pairing energy of 0.69 MeV in the effective excitation was considered for the level density of ^{239}U. Using the transmission coefficients in table 4 together with eq. (5), results in $D_0 = 22.20$ eV and $\overline{\Gamma}_\gamma(\ell = 1) = 22.5$ meV. The level spacing derived for the two cases are within the uncertainties consistent with the value $D_0 = (21.19 \pm 0.55)$ eV that was derived from a statistical analysis of resolved resonance parameters by Derrien *et al.* [43] and Courcelle *et al.* [7]. Both versions have shown almost the same cross sections and very similar behaviour in the interpretation of benchmark experiments, since they retain the fitted capture transmission coefficients practically intact. The second version has ultimately been chosen for the final evaluation.

The file produced in this work is taken over in the CIELO file that is produced at the IAEA [13], referred to as CIELO(IAEA), and adopted in ENDF/B-VIII.0 [54]. However, it was not considered for the latest version of the JEFF project, which is referred to as JEFF-3.3T4 [55].

The cross sections obtained in this work are shown in fig. 5 and fig. 6 and compared with those recommended in ENDF-B-VII.1, JENDL-4, JEF-2.2, JEFF-3.2 and JEFF-3.3T4. These figures show that there is a substantial difference between the capture cross section obtained in this work and the one recommended in JEFF-3.3T4. The capture cross section in JEFF-3.3T4 is in the region between 10 keV and 150 keV on average lower by $\sim 5\%$. There is also a difference between the cross sections recommended in the previous versions of the JEFF-library (*i.e.*, JEF-2.2 and JEFF-3.2) and the one in JEFF-3.3T4. Most probably these differences are due to adjustments of nuclear data to results of integral benchmark experiments.

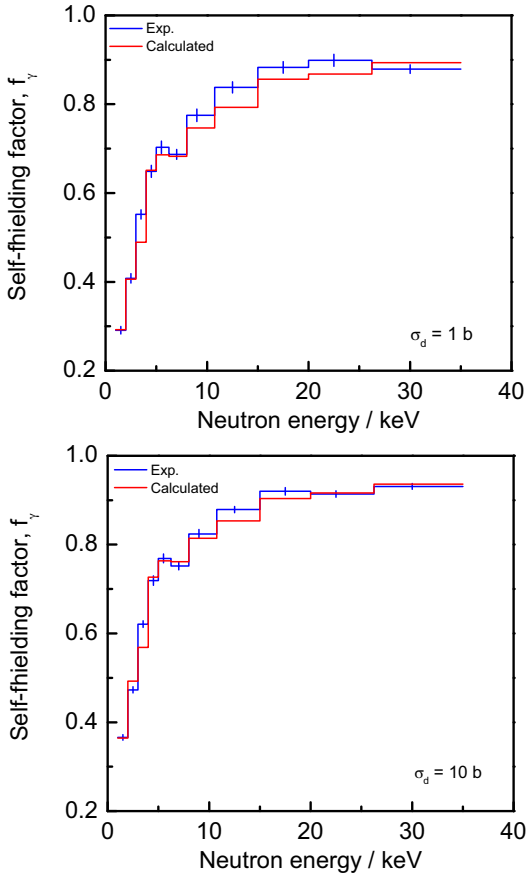

Fig. 8. Capture self-shielding factors f_γ for dilution cross sections $\sigma_d = 1$ b and $\sigma_d = 10$ b. The experimental data of Oigawa *et al.* [61] are compared with the factors derived from the evaluated URR file presented in this work complemented with the resolved resonance parameters of the CIELO file.

A systematic analysis of the CIELO(IAEA) and JEFF-3.3T4 files was performed based on the results of the BigTen benchmark experiment. This experiment, which is fully documented in the ICSBEP Handbook [56] with reference IMF-007, shows a high sensitivity to the ^{238}U(n, γ)

cross section in the URR. In case of the BigTen experiment, a decrease of the capture cross section for ^{238}U(n, γ) in the URR by $\sim$ 5% results in an increase of k_{eff} of $\sim$ 500 pcm. The reduced capture cross section for ^{238}U(n, γ) in the JEFF-3.3T4 evaluation is mainly compensated by an increasing cross section for ^{235}U(n, γ). A more detailed discussion on the difference with the ^{238}U(n, γ) cross section in JEFF-3.3T4 and the compensating effects is being prepared [57].

5 Validation of the ENDF-6 file

The file recommended in this work has been validated by a comparison with results of both spectrum averaged cross section measurements and energy dependent self-shielding factor (Bondarenko) experiments for the capture reaction.

The total cross section in table 2 is consistent with results of measurements at filtered neutron beams with neutron energies of $\sim$ 54 keV and 144 keV reported in refs. [48,58]. Calculated spectrum averaged cross sections were derived by combining the data in table 2 with the cross section taken from the CIELO project for energies below 20 keV and above 150 keV [13]. The neutron energy distributions were obtained from calculations that were validated by results of experiments with a hydrogen proportional counter [59]. The calculated values, reported in table 5, are within the uncertainties in full agreement with those measured by Pham *et al.* [58]. The calculated average total cross section for the 144 keV beam is not in full agreement with the value determined by Litvinsky *et al.* [48]. This can be due to the spectrum used in the calculations or to an underestimation of the uncertainty quoted by Litvinsky *et al.* [48].

The average capture cross section $\overline{\sigma}_\gamma$ recommended in this work can be compared with the spectrum averaged cross section reported by Wallner *et al.* [60]. The latter was obtained from a combination of activation measurements and atom counting of the reaction products using accelerator mass spectrometry. For a neutron beam with a distribution that is very similar to a Maxwell-Boltzman distribution of $kT \sim 25.3$ keV they derived a spectrum averaged ^{238}U(n, γ) cross section of (391 ± 17) mb [60]. This value is within the uncertainties in agreement with the average value of (400 ± 5) mb derived from the data in table 3 complemented by the CIELO file for energies below 5 keV and above 150 keV. For the calculations the spectrum reported in the EXFOR library was used.

The compensating effect in JEFF-3.3T4 mentioned in sect. 4 can be confirmed by comparing the experimental capture cross section ratio $R = {}^{238}\mathrm{U}(\mathrm{n},\gamma)/{}^{235}\mathrm{U}(\mathrm{n},\gamma)$ obtained by Wallner *et al.* [60] for an average energy of $\sim$ 25.3 keV with the one derived from the CIELO(IAEA) and JEFF-3.3T4 files. Using the energy distribution reported in the EXFOR data library, a ratio of $R_{CIELO} = 0.57$ is obtained from the CIELO(IAEA) file [13,15]. This ratio is within the uncertainty in agreement with the experimental value of $R_{exp} = 0.60 \pm 0.03$ [60]. The ratio of $R_{JEFF\text{-}3.3T4} = 0.49$ derived from the JEFF-3.3T4 file is smaller by almost 20%, while the experimental uncertainty is less than 5%. This underestimation is due to the combined decrease of the ^{238}U(n, γ) cross section and increase of the ^{235}U(n, γ) cross section in JEFF-3.3T4. The same ratios are obtained using a Maxwellian energy distribution with $kT = 25.3$ keV for the calculation of the spectrum averaged cross sections. The ratio is also independent of any reference to a standard reaction cross section.

Experimental self-shielding factors f_γ for the ^{238}U (n, γ) reaction have been deduced from a series of transmission and self-indication measurements by Oigawa *et al.* [61]. Figure 8 shows the good agreement between the experimental data of Oigawa *et al.* [61] and the self-shielding factors calculated with NJOY using the file presented in this work. Note that the calculated values below 20 keV are based on the CIELO file in the resolved resonance region [13,15]. This file was constructed by replacing the parameters derived by Derrien *et al.* [43] below 1200 eV with those of Kim *et al.* [10].

A test of the ^{238}U evaluated data file based on results of integral benchmark experiments is reported by Capote *et al.* [13] and Chadwick *et al.* [15].

6 Summary

An ENDF-6 compatible evaluation of average resonance parameters and dilute average cross sections for neutron interactions with ^{238}U in the energy region from 5 keV to 150 keV has been carried out using only energy dependent microscopic cross section data. Average total and capture cross sections have been derived from a least squares analysis to experimental cross section data. They have been parameterised in terms of average resonance parameters maintaining consistency with results of optical model calculations based on a dispersive coupled channel optical model potential. The average parameters derived from a least squares adjustment to the average total and capture cross sections are within the uncertainties fully consistent with the parameters derived from a statistical analysis of resolved resonance parameters. The average cross sections and average resonance parameters have been used to produce an ENDF-6 compatible evaluated file for neutron interactions with ^{238}U in the unresolved resonance region. The evaluation has been validated by results of both spectrum averaged cross section measurements and self-shielding factor experiments.

This work was supported by the European Commission through the EUFRAT project of the JRC Geel (BE) and by the CIELO project co-ordinated by the Nuclear Data Section of the IAEA and the Nuclear Energy Agency of the OECD.

References

1. S. Kopecky, I. Sirakov *et al.*, *Status of evaluated data files for* ^{238}U *in the resonance region*, JRC Technical Report, EUR 27504 EN (2015).
2. F.H. Fröhner, Nucl. Sci. Eng. **103**, 119 (1989).
3. F.H. Fröhner, Nucl. Sci. Eng. **111**, 404 (1992).
4. A.D. Carlson, V.G. Pronyaev, D.L. Smith, N.M. Larson, Z. Chen, G.M. Hale, F.-J. Hambsch, E.V. Gai, Soo-Youl Oh, S.A. Badikov, T. Kawano, H.M. Hofmann, H. Vonach, S. Tagesen, Nucl. Data Sheets **110**, 3215 (2009).
5. J.A. Harvey, N.W. Hill, F.G. Perey, G.L. Tweed, L. Leal, *High-resolution neutron transmission measurements on* ^{235}U*,* ^{239}Pu*, and* ^{238}U, in *Proceedings of the International Conference on Nuclear Data for Science and Technology, Mito, Japan, 30 May-3 June, 1988* (JAERI, 1998) pp. 115–118.
6. V.M. Maslov, Yu.V. Porodzinskij, M. Baba, A. Hasegawa, Ann. Nucl. Energy **29**, 1707 (2002).
7. A. Courcelle, H. Derrien, L.C. Leal, N.M. Larson, Nucl. Sci. Eng. **156**, 391 (2007).
8. H. Derrien, J.A. Harvey, K.H. Guber, L.C. Leal, N.M. Larson, *Average neutron total cross sections in the unresolved resonance energy range from ORELA high-resolution transmission measurements*, ORNL/TM-2003/291, Oak Ridge National Laboratory (2004).
9. J.L. Ullmann, T. Kawano, T.A. Bredeweg, A. Couture, R.C. Haight, M. Jandel, J.M. O'Donnell, R.S. Rundberg, D.J. Vieira, J.B. Wilehlmy, J.A. Becker, A. Chyzh, C.Y. Wu, B. Baramsai, G.E. Mitchell, M. Krtička, Phys. Rev. C **89**, 034603 (2014).
10. H.I. Kim, C. Paradela, I. Sirakov, B. Becker, R. Capote, F. Gunsing, G.N. Kim, S. Kopecky, C. Lampoudis, Y.-O. Lee, R. Massarczyk, A. Moens, M. Moxon, V.G. Pronyaev, P. Schillebeeckx, R. Wynants, Eur. Phys. J. A **52**, 170 (2016).
11. n_TOF Collaboration (F. Mingrone *et al.*), Phys. Rev. C **95**, 034604 (2017).
12. n_TOF Collaboration (T. Wright *et al.*), *Measurement up to 80*keV *of the* ^{238}U(n,γ) *Cross Section with the TAC at the CERN n_TOF Facility*, to be published in Phys. Rev. C.
13. R. Capote, A. Trkov *et al.*, *Evaluation of neutron-induced reactions on* ^{235}*U and* ^{238}*U targets up to 30*MeV, to be published in Nucl. Data Sheets (2018).
14. M.B. Chadwick, E. Dupont *et al.*, Nucl. Data Sheets **118**, 1 (2014).
15. M.B. Chadwick, R. Capote *et al.*, *CIELO Collaboration Summary Results: International Evaluations of Neutron Reactions on Uranium, Plutonium, Iron and Oxygen*, to be published in Nucl. Data Sheets (2018).
16. W.P. Poenitz, *Data interpretation, objective, evaluation procedures and mathematical technique for the evaluation of energy-dependent ratio, shape and cross section data*, in *Proceedings of the Conference on Nuclear Data Evaluation Methods and Procedures*, BNL-NCS-51363 (Associated Universities INC, 1981), pp. 249–290.
17. `https://www-nds.iaea.org/standards/codes.html`.
18. J.F. Whalen, A.B. Smith, *Uranium total cross section*, Argonne National Laboratory report series No. 7710 (1971) p. 9, EXFOR entry = 10009.
19. V.N. Kononov, E.D. Poletaev, *Measurement of the total cross-section and resonance self-shielding capture cross-section for U-238 for 5–80*keV *neutrons*, in *Proceedings of the 2nd National Soviet Conference on Neutron Physics, Kiev, 28 May - 1 June 1973*, Vol. **2** (FEI Obninsk, 1974) pp. 195–205 (Russian), EXFOR entry = 40328.
20. W.P. Poenitz, J.F. Whalen, A.B. Smith, Nucl. Sci. Eng. **78**, 333 (1981), EXFOR entry = 10935.
21. W.P. Poenitz, J.F. Whalen, *Neutron total cross section measurements in the energy region from 47*keV *to 20*MeV, ANL/NDM-80, Argonne National Laboratory (1983).
22. I. Tsubone, Y. Nakajima, Y. Furuta, Nucl. Sci. Eng. **88**, 579 (1984), EXFOR entry = 21813.
23. M.V. Bokhovko, V.N. Kononov, G.N. Manturov, E.D. Poletaev, V.V. Sinitsa, A.A. Voevodskij, *Measurement and analysis of neutron transmission and self-indication of the neutron radiative capture cross-section for* ^{238}U *in the 5–110*keV *energy region*, IAEA Report, INDC(CCP)-322 (1990), EXFOR entry = 41016.
24. N. Otuka, E. Dupont *et al.*, Nucl. Data Sheets **120**, 272 (2014).
25. M.C. Moxon, M.G. Sowerby, J.B. Brisland, ^{238}U *resolved resonance parameters*, in *Proceedings of the International Conference on Physics of Reactors, Operation, Design and Computation, PHYSOR'90 Marseille, 23–27 April 1990* (1990) pp. III 41–51.
26. S.A. Badikov, Chen Zhenpeng, A.D. Carlson, E.V. Gai, G.M. Hale, F.-J. Hambsch, H.M. Hofmann, T. Kawano, N.M. Larson, V.G. Pronyaev, D.L. Smith, Soo-Youl Oh, S. Tagesen, H. Vonach, *International evaluation of neutron cross-section standards*, IAEA Report, STI/PUB/1291, pp. 1–173 (2007).
27. C. Massimi, B. Becker, E. Dupont, S. Kopecky, C. Lampoudis, R. Massarczyk, M. Moxon, V. Pronyaev, P. Schillebeeckx, I. Sirakov, R. Wynants, Eur. Phys. J. A **50**, 124 (2014).
28. n_TOF Collaboration (C. Lederer *et al.*), Phys. Rev. C **83**, 034608 (2011).
29. L. Dresner, *Resonance Absorption in Nuclear Reactors* (Pergamon Press, Elmsford, New York, 1960).
30. P.A. Moldauer, Nucl. Phys. A **344**, 185 (1980).
31. H.M. Hofmann, J. Richert, J.W. Tepel, H.A. Weidenmüller, Ann. Phys. **90**, 403 (1975).
32. J.J.M. Verbaarschot, H.A. Weidenmüller, M.R. Zirnbauer, Phys. Rep. **129**, 367 (1985).
33. H. Henryson, B.J. Toppel, C.G. Sternberg, *MC*^{2}*-II: A code to calculate fast neutron spectra and multigroup cross sections*, Argonne National Laboratory Report ANL-8144, ENDF-239 (1976).
34. I. Sirakov, R. Capote, F. Gunsing, P. Schillebeeckx, A. Trkov, Ann. Nucl. Energy **35**, 1223 (2008).
35. I. Sirakov, B. Becker, R. Capote, E. Dupont, S. Kopecky, C. Massimi, P. Schillebeeckx, Eur. Phys. J. A **49**, 144 (2013).
36. R. Capote, A. Trkov, M. Sin, M. Herman, A. Daskalakis, Y. Danon, Nucl. Data Sheets **118**, 26 (2014).
37. J.M. Quesada, R. Capote, E.Sh. Soukhovitskii, S. Chiba, Nucl. Data Sheets **118**, 270 (2014).
38. E.Sh. Soukhovitskiĭ, R. Capote, J.M. Quesada, S. Chiba, D.S. Martyanov, Phys. Rev. C **94**, 64605 (2016).
39. E.Sh. Soukhovitskiĭ, S. Chiba, O. Iwamoto, K. Shibata, T. Fukahori, G. Mororovskij, *Programs OPTMAN and SHEMMAN Version 8 (2004)*, JAERI-Data/Code 2005-002 (Japan Atomic Energy Agency, 2005).
40. E.Sh. Soukhovitskiĭ, S. Chiba, R. Capote, J.M. Quesada, S. Kunieda, G. Mororovskij, *Supplement to OPTMAN Code,*

Manual Version 10 (2008), JAEA-Data/Code 2008-025 (Japan Atomic Energy Agency, 2008).
41. M. Herman, R. Capote, B.V. Carlson, P. Obložinský, M. Sin, A. Trkov, H. Wienke, V. Zerkin, Nucl. Data Sheets **108**, 2655 (2007).
42. R. Capote, M. Herman, P. Obložinský, P.G. Young, S. Goriely, T. Belgya, A.V. Ignatyuk, A.J. Koning, S. Hilaire, V.A. Plujko, M. Avrigeanu, O. Bersillon, M.B. Chadwick, T. Fukahori, Zhigang Ge, Yinlu Han, S. Kailas, J. Kopecky, V.M. Maslov, G. Reffo, M. Sin, E.Sh. Soukhovitskii, P. Talou, Nucl. Data Sheets **110**, 3107 (2009).
43. H. Derrien, L.C. Leal, N.M. Larson, A. Courcelle, *Neutron resonance parameters and calculated cross sections from Reich-Moore analysis of experimental data in the neutron energy range from 0 to 20* keV, ORNL/TM-2005/241, Oak Ridge National Laboratory (2005).
44. T. Kawano, R. Capote, S. Hilaire, P. Chau Huu-Tai, Phys. Rev. C **94**, 014612 (2016).
45. G.H.R. Kegel, L.E. Beghian, G.P. Couchell, J.J. Egan, T.V Marcella, A. Mittler, D.J. Pullen, W.A. Schier, E. Sheldon, M.A. Doyle, S. Jain, J. Menachery, S. Mathew, N.B. Sullivan, A. Wang, *Neutron scattering on heavy deformed nuclei*, DOE-NDC-12 (1978) pp. 151–152, EXFOR entry = 14019.
46. F.Y. Tsang, R.M. Brugger, Nucl. Sci. Eng. **65**, 70 (1978), EXFOR entry = 10696.
47. R.R. Winters, N.W. Hill, R.L. Macklin, J.A. Harvey, D.K. Olsen, G.L. Morgan, Nucl. Sci. Eng. **78**, 147 (1981), EXFOR entry = 10998.
48. L.L. Litvinskii, V.P. Vertebnyi, V.A. Libman, A.V. Murzin, Sov. At. Energy **62**, 241 (1987), EXFOR entry = 40924.
49. M.C. Moxon, J.A. Wartena, H. Weigmann, G.J. Vanpraet, *Inelastic neutron scattering from U-238*, in *Proceedings of the International Conference on Nuclear Data for Science and Technology, Gatlinburg 1994 (USA)* (American Nuclear Society, 1994) pp. 981–983, EXFOR entry = 22329.
50. I. Sirakov *et al.*, in preparation (2018).
51. A. Trkov, private communication (2017).
52. R.E. Slovacek, D.S. Cramer, E.B. Bean, J.R. Valentine, R.W. Hockenbury, R.C. Block, Nucl. Sci. Eng. **62**, 455 (1977), EXFOR entry = 10567.
53. J.A. Holmes, S.E. Woosley, W.A. Fowler, B.A. Zimmerman, At. Data Nucl. Data Tables **18**, 305 (1976).
54. D.A. Brown, M.B. Chadwick *et al.*, *ENDF/B-VIII.0: The eighth major library release of nuclear reaction data with new standards and CIELO-project cross sections*, to be published in Nucl. Data Sheets (2018).
55. O. Cabellos, F. Michel-Sendis, *Testing JEFF-3.3T4 in ICSBEP benchmarks*, JEFF meeting 24–27 April 2017, JEF/DOC-1843 (2017), `http://www.oecd-nea.org/dbdata/jeff-beta/JEFF33T4/neutrons/`.
56. ICSBEP Working Group, *International Handbook of Evaluated Criticality Safety Benchmark Experiments*, NEA/NSC/DOC(95)03 (Nuclear Energy Agency, OECD, 2009).
57. B. Kos, I. Kodeli, P. Schillebeeckx, G. Žerovnik, in preparation.
58. Pham Zuy Hien, Vuong Huu Tan, Nguyen Phuoc Xuan, *Total neutron cross-section of U-238 as measured with filtered neutrons of 55 and 144* keV, IAEA Report, INDC(NDS)-265 (1992), EXFOR entry = 31457.
59. O. Gritzay, private communication (2017).
60. A. Wallner, T. Belgya, M. Bichler, K. Buczak, F. Käppeler, C. Lederer, A. Mengoni, F. Quinto, P. Steier, L. Szentmiklosi, Phys. Rev. Lett. **112**, 192501 (2014), EXFOR entry = 23170.
61. H. Oigawa, Y. Fujita, K. Kobayashi, S. Yamamoto, I. Kimura, J. Nucl. Sci. Technol. **28**, 879 (1991).